Response to reviewers for "Gas-particle partitioning, molecular weight, and yield of organic nitrate under different urban VOC, NO_x, and oxidation conditions during SAPHIR-CHANEL campaign" by Farhan R. Nursanto, Quanfu He, Sophia van de Wouw, Annika Zanders, Thorsten Hohaus, Willem S. J. Kroese, Robert Wegener, Max Gerrit Adam, Benjamin Winter, René Dubus, Lukas Kesper, Franz Rohrer, Yuwei Wang, Emily Matthews, Aristeidis Voliotis, Thomas J. Bannan, Gordon McFiggans, Hugh Coe, Yizhen Wu, Milan Roska, Manjula Canagaratna, Mitch Alton, Matthew M. Coggon, Chelsea E. Stockwell, Kelvin H. Bates, Eva Y. Pfannerstill, Sören R. Zorn, Hui Wang, Matthieu Riva, Sebastien Perrier, Boxing Yang, Lu Liu, Anna Novelli, Michelle Färber, Hendrik Fuchs, Andrea Carolina Marcillo Lara, Achim Grasse, Christian Wesolek, Ralf Tillmann, Rupert Holzinger, Maarten C. Krol, Georgios I. Gkatzelis, and Juliane L. Fry.

(Manuscript ID: EGUSPHERE-2025-6310)

We appreciate the anonymous referees for their detailed and constructive feedback on our manuscript. The valuable suggestions have significantly improved this revised version. To guide the review process, we have copied the reviewer comments in black text, renumbered for each reviewer to facilitate cross-referencing. Our responses are provided in regular blue text, and we have responded to all the referee's comments and made alterations to our paper in **bold text**. In black text, line/figure/table number refers to the number in the submitted preprint, while in blue text, line number refers to the line in the updated version of the manuscript. The black text in the response also shows the unchanged part of the manuscript. New terms or abbreviations from this revision are added into Appendix A.

—

Response to RC1 (Anonymous Referee #1): https://doi.org/10.5194/egusphere-2025-6310-RC1

This manuscript reports a set of SAPHIR-CHANEL chamber experiments and investigated the bulk organic nitrate formation, molar yield, and partitioning. A range of biogenic and urban VOC-NO_x mixtures under daytime and nighttime conditions were investigated. The day-night differences was interpreted using a combination of online mass spectrometers. Overall, this study is well designed and the paper provided comprehensive analysis to support their conclusion. However, there are still some placpes I feel the authors can improve and need some additional clarifications. Therefore, I suggest a minor revision.

Major comments (RC1-M):

RC1-M-1. The day-night interpretation considered both temperature/RH difference and chemical composition change. The impact from two major causes were not separated.

The discussion mentioned that lower temperature and higher RH in nighttime experiments enhanced partitioning, thus increasing C_p/C_g. At the same time, more dimers were identified at nighttime samples, implying composition changes. While these two could both be true, it would be better if the impact from temperature/RH could be separated with that from chemical composition/oxidation regime.

We thank the reviewer for this comment. As similar questions are asked in the other comments, the impact from temperature and RH is detailed in the response to RC1-M-2 and RC1-M-3, respectively.

More discussion about the differences in chemical composition between daytime and nighttime experiments with comparable temperature condition would be helpful.

We compared the daytime and nighttime experiments at temperatures between 24 ºC and 27 ºC when discussing $K_{p,ON}$ but we did not further formulate the chemical differences between the two. We updated the manuscript as response to this comment as follows:

We updated the text as follows:

L473-479 → **L583-597**

> ***<< enter new line >>***
>
> Furthermore, when we examine the $K_{p,ON}$ values at temperatures between 24 ºC and 27 ºC, for which both daytime and nighttime experiments were conducted, we see that the trend of higher $K_{p,ON}$ for nighttime experiments compared to daytime experiments still holds for similar temperatures. The uncertainty range also overlaps minimally between the $K_{p,ON}$ values. This ~~indicates~~**reiterates** that the difference in $K_{p,ON}$ between nighttime and daytime conditions is due not only to temperature differences, but also to actual differences in chemical pathways~~leading to the production of lower volatility and more oxygenated ON compounds under nighttime conditions~~.
>
> **Under daytime conditions, NO concentrations are relatively high, and small alkenes and other short-chain VOCs react with $OH^{\cdot}$ to form short-chain $RO_2^{\cdot}$. As a result, the long-chain $RO_2^{\cdot}$+$RO_2^{\cdot}$ pathway is likely minor relative to reactions of long-chain $RO_2^{\cdot}$ with short-chain $RO_2^{\cdot}$, NO, and $HO_2^{\cdot}$. Even in the daytime limonene experiment, where we have only C_{10} as precursor, C_{10} $RO_2^{\cdot}$ is more likely to react with NO_x to form ON than to undergo dimerization (see Fig. 6a), leading to fewer high-molecular-weight ON compounds, thus resulting in lower $K_{p,ON}$.**
>
> **In contrast, the nighttime $RO_2^{\cdot}$ formation in the Los Angeles VOC precursor mixture is likely to be produced mainly from high-carbon unsaturated VOCs (e.g., monoterpenes), which can produce long-chain $RO_2^{\cdot}$ that undergo dimerization under near-zero NO conditions (Fig. 6f). However, these dimers are not observed in the gas phase, possibly because they rapidly condense into particles or are lost during sampling. Oxidation by $NO_3^{\cdot}$ also may occur with primary oxidation products to form more oxidized organic nitrates with lower volatility (Guo et al., 2022), which also increases $K_{p,ON}$.**

L555-557 → **L681-685**

> The observed gas-particle partitioning coefficient, when treated as a bulk compound at equilibrium, shows that the bulk organic nitrate is comparable to the calculated values of monoterpene-related species using SIMPOL.1 method (**$K_{p,ON}$ from** 10^{-4} to 10^{-2} m^3 μg^{-1} at 18–40 °C), regardless of the complexity of the mixture. **Nighttime oxidation produces bulk ON with lower O:C ratio and volatility (lower C_{ON}^*, higher $K_{p,ON}$) due to the higher degree of dimerization compared to the daytime oxidation.** However, future studies …

RC1-M-2. Temperature effects should be quantified (e.g. Clausius-Clapeyron equation), while currently temperature is used as a post-hoc explanation rather than a tested hypothesis.

Given that K_p is temperature dependent and Fig. 6 explicitly plot $K_{p,ON}$ versus T, a straightforward expectation is to apply a Clausius-Clapeyron correction/sensitivity analysis to test whether the observed day-night offsets are consistent with thermodynamics alone.

We performed a sensitivity analysis using the Clausius-Clapeyron equation of experiments with VOC precursors that are performed under both daytime and nighttime conditions (limonene, VCPs, Los Angeles replicas). We updated the manuscript as follows:

Section 2.5

L314 → **L362-375,** new paragraph inserted as part of **Section 2.5.2**

> **Furthermore, we characterized the influence of temperature (T) using the enthalpy of vaporization (ΔH_{vap}) of bulk organic nitrates from Clausius-Clapeyron equation (see Eq. 9). To determine whether any observed $K_{p,ON}$ differences between two experimental conditions (e.g., daytime vs. nighttime) are purely due the temperature differences, the observed ΔH_{vap} can be compared with the expected ΔH_{vap} for organic nitrates or SOA from other studies; 30–150 kJ mol^{-1} for a volatility range of organic compounds (Pankow and Asher, 2008; Epstein et al., 2010). A discrepancy between the observed ΔH_{vap} and expected ΔH_{vap} suggests that the observed $K_{p,ON}$ offset is influenced by parameters other than temperature, such as chemical composition (observed ΔH_{vap} > expected ΔH_{vap}) or kinetic limitations (observed ΔH_{vap} < expected ΔH_{vap}).**
>
> $$\ln\left(\frac{K_{p,ON;N}}{K_{p,ON;D}}\right) = \frac{\Delta H_{vap}}{R} \cdot \left(\frac{1}{T_N} - \frac{1}{T_D}\right) \quad (9)$$
>
> **$K_{p,ON;N}$: gas-particle partitioning coefficient of organic nitrates under nighttime conditions (m^3 μg^{-1})**
> **$K_{p,ON;D}$: gas-particle partitioning coefficient of organic nitrates under daytime conditions (m^3 μg^{-1})**
> **ΔH_{vap}: enthalpy of vaporization (kJ mol^{-1})**
> **R: ideal gas constant ($8.314 \cdot 10^{-3}$ kJ K^{-1} mol^{-1})**
> **T_N: temperature under nighttime conditions (K)**
> **T_D: temperature under daytime conditions (K)**

Section 3.3.3. Observed vs. theoretical gas-particle partitioning coefficient ($K_{p,ON}$)

L468-473 → **L566-582**

> We found that the nighttime experiments of limonene precursor, VCP mixtures, Los Angeles emission profile, and Los Angeles anthropogenic+biogenic emission profile have higher **mean** $K_{p,ON}$ values, **$(6.1\pm3.2)\cdot10^{-3}$ m^3 μg^{-1} at T = 295±3 K (mean±standard deviation)** compared to the daytime experiments with the same

precursor, **$(9.1\pm3.6)\cdot10^{-4}$ m^3 μg^{-1} at T = 303±5 K**. Similarly to the trend of the particle-to-gas ratio, ~~since~~ lower chamber temperatures and higher RHs under nighttime conditions ~~enhance~~**increase aerosol liquid water content, and thus** the condensation of chemical species to the particle phase **and the aqueous-phase chemistry**.

This may seem biased since the daytime experiments are never done at lower temperature (and vice versa). However, ~~we highlight that~~ **because** nighttime temperatures are lower than daytime temperatures in the real world~~ as well, so that,~~ these results represent realistic scenarios. **The Clausius-Clapeyron sensitivity analysis using $K_{p,ON}$ values under daytime and nighttime conditions of the same VOC precursor mixtures suggests that the daytime-nighttime $K_{p,ON}$ difference is not solely due to temperature. The daytime-nighttime $K_{p,ON}$ difference, if solely driven by temperature, would produce a ΔH_{vap} of ~170 kJ mol^{-1}. This value is higher than the range of ΔH_{vap} values for semi-volatile organic compounds, 70–120 kJ mol^{-1} for the volatility range of $1 < \log(C_i^*) < 4$ (Pankow and Asher, 2008; Epstein et al., 2010). This confirms that the daytime-nighttime $K_{p,ON}$ differences are not driven solely by vaporization thermodynamics, but rather due to different particle chemical composition. Under nighttime conditions, the particles contain much less volatile nitrates and higher molecular weight compounds compared to daytime conditions that modify the physical properties of the aerosol phase, decreasing its volatility and thus increasing the nighttime $K_{p,ON}$. This daytime-nighttime ΔH_{vap} and $K_{p,ON}$ offsets is consistent with WALL-E observations showing higher signal contribution from dimers in the particle phase in the nighttime experiments (Fig. 6).**

RC1-M-3. The impact of RH is mentioned together with temperature, but no mechanistic explanation is provided (i.e. water uptake, aqueous chemistry)

More discussion about how does RH impact partitioning would be helpful. Either through higher aerosol liquid water increases absorptive capacity or potential aqueous phase/heterogeneous chemistry leads to dimer formation.

While RH may partially influence the phase partitioning as we have stated throughout the manuscript, we would not like to emphasize RH as a very important factor in determining the gas-particle partitioning. We kept the initial relative humidity similar across experiments and the change of RH are not drastic between experiments after the SOA formation has peaked. The phase partitioning is mostly driven by vapor pressure, and the influence of RH also requires further study to show how the aerosol liquid water content influence the organic nitrate formation. We added one mechanistic explanation of the RH influence to the phase partitioning as follows.

L366-367 → **L438-443**

The difference can be partially explained by lower temperature and higher RH during nighttime experiments, which promote the condensation of ON that increases its mass fraction. Lower temperature increases the particle partitioning of semivolatile species, and **higher RH increases the aerosol liquid water content, which enhances the absorptive capacity of the particle phase for soluble organic nitrates. It also enables aqueous-phase and heterogeneous chemistry that facilitates the formation of low-volatility dimers, increasing $pRONO_2$ mass fraction in the organic aerosol phase. This change in chemistry affects the $pRONO_2$ ~~Associated with their~~** molecular weight~~,~~**.** ~~n~~**N**ighttime $NO_3^{\cdot}$ chemistry results in higher ON production with heavier compounds compared to daytime $OH^{\cdot}$ chemistry…

RC1-M-4. Photochemical condition (i.e. solar flux, J-values) are not provided. Day-night conditions differ majorly in chemical reaction pathway, especially the radical production pathway. It would be helpful for this manuscript to provide photolysis metrics (e.g. solar flux), as it is an important experimental parameter when interpreting daytime oxidation.

We have added the j_{NO2} values for the experiments under daytime conditions to complement the information in Table 1. The average value of j_{NO2} throughout the campaign is 4.2E-03 s^{-1}. For the nighttime experiment, the chamber roof shutter is closed, thus the j_{NO2} is assumed zero.

We updated Table 1 in the manuscript as follows:

L104 (Table 1) → **L101 (Table 1, as shown below)**

Table 1. List of experiments in the SAPHIR-CHANEL 2024 campaign included in this paper, grouped based on VOC precursors. **The average photolysis rate coefficient of NO_2 (j_{NO2} , in s^{-1}) is provided for each experiment under daytime conditions; nighttime experiments assume j_{NO2} = 0.** All experiments were run at initially 60 % relative humidity (RH), unless indicated otherwise.

Date (yyyy.mm.dd)	VOC precursor(s)	Oxidation and NO conditions	j_{NO2} (s^{-1})
Single-compound precursor experiments			
2024.07.01	limonene	daytime, low NO	3.6E-03
2024.07.03[a]	limonene	nighttime	-
Source-specific emission mixture experiments			
2024.07.04	VCPs	daytime, low NO	4.1E-03
2024.07.08	VCPs	daytime, medium NO	3.7E-03
2024.07.09	VCPs	daytime, high NO	4.5E-03
2024.07.05	VCPs	nighttime	-
2024.07.17	diesel	daytime, medium NO	3.3E-03
2024.07.18	diesel	daytime, high NO	4.4E-03
2024.07.11	gasoline	daytime, medium NO	3.3E-03
2024.07.10	gasoline	daytime, high NO	4.3E-03
2024.07.16	cooking	daytime, low NO	4.0E-03
2024.07.15	cooking	daytime, medium NO	4.6E-03
Complex urban mixture experiments			
2024.07.22	Los Angeles anthropogenic emission	daytime, medium NO	4.7E-03
2024.07.23	Los Angeles anthropogenic emission	nighttime	-
2024.08.05	Los Angeles anthropogenic+biogenic emission (+O_3)	daytime, low NO	4.0E-03
2024.07.29	Los Angeles anthropogenic+biogenic emission	daytime, medium NO	4.9E-03
2024.08.06	Los Angeles anthropogenic+biogenic emission (+O_3+NO_2)	daytime, high NO	4.1E-03
2024.07.31	Los Angeles anthropogenic+biogenic emission	nighttime	-
2024.07.30	global city anthropogenic emission	daytime, medium NO	4.6E-03
2024.08.02	future city anthropogenic+biogenic emission	daytime, low NO	4.2E-03
Background experiments			
2024.07.28	background (no seed)	daytime	4.9E-03
2024.08.04	background (with seed)	daytime	3.2E-03

[a] Initial RH 20 %.

RC1-M-5. The manuscript attributes the higher nighttime limonene $K_{p,ON}$ to enhanced dimer formation. However, the SIMPOL-based comparison in Fig. 6 did not include any monoterpene dimer candidates, and the nighttime limonene SOA fall into the range of limonene monomer. Representative monoterpene dimer candidates should be included in Fig. 6.

Monoterpene dimer candidates are indeed not shown in the plot in Fig. 6 **(now Fig. 7)**. However, we provided one of the monoterpene nitrate dimer (shown in the lower left of the figure) which has a theoretical $K_{p,ON}$ value of 1.1E+04 at 25 ºC as a guide for the reader to its value. This value is significantly higher compared to the rest of the compounds shown in the plot. We found that it would squeeze the details of the other monoterpene nitrate compounds if we extended the y-axis range up to 10^4 m^3 μg^{-1}; therefore, we decided to only show it at the bottom of the figure.

While it is true that limonene dimers are produced, the limonene monomers are likely still the majority of the product. Therefore, the dimers produced under nighttime conditions do not increase the bulk $K_{p,ON}$ greatly compared to the daytime limonene experiment, but not high enough to move the nighttime limonene SOA up in the scale into the range of limonene dimers. While WALL-E observations suggest that the $C_{>10}$ compounds represent 15–48 % of the total signal, these are based on the total signal intensity, not sensitivity-based mass concentration of the compounds. Meanwhile, $K_{p,ON}$ is calculated based on calibrated measurements of NO_3 from AMS, total NO_y, NO_x, HONO, and HNO_3 from MR-CIMS. Based on Gao et al. (2025), the mass fraction contribution of dimers to the particle phase composition they found in their study (14-18 %) is about lower compared to the signal-based contribution (23-29 %). This means that signal-based fraction can overestimate the contribution of dimers to bulk pON concentration.

We added this information to the manuscript:

L443-448 → **L533-536**

> In addition to species related to monoterpene compounds (carbon number 6–10), substantial signal fraction is observed for monoterpene dimers (carbon number 15–20) in the particle phase, where it represents 15–48 % of the total signal. **A recent study showed that the mass fraction contribution of dimers was about a factor of 2 lower compared to its signal fraction (Gao et al., 2025)**. ***<<new line entered>>***

L523 → new paragraph inserted, becomes **L640-645**

> **Although WALL-E observations suggest that the $C_{>10}$ compounds represent higher fraction of the total signal in the particle phase in the nighttime experiments, the observed nighttime $K_{p,ON}$ values do not approach theoretical $K_{p,ON}$ values of dimers, likely due to the mass dominance of monomer nitrates. The dimer contribution fraction from WALL-E in this study is based on the total signal intensity, while the values of $K_{p,ON}$ are determined based on calibrated mass concentrations from total NO_y and AMS instruments. In addition, a structure-independent volatility estimation for the assigned molecular formulas (e.g., formula-based C*/2D VBS mapping) could provide more information of whether the nighttime experiments formed lower volatile compounds.**

We thank the reviewer for this suggestion. We have plotted the 2D-VBS mapping below following Donahue et al. (2011), with parameterizations following Stolzenburg et al. (2018). Unlike AMS that includes the organic moiety of both nitrogen-containing and non-nitrogen-containing organics but not the nitrate moiety, we used the O:C ratio from nitrogen-containing masses ($C_xH_yO_zN_k$) signal detected by WALL-E. This is to include only organic nitrogen compounds (organic+nitrate moiety) and exclude non-nitrogen functionalized organics, matching the gas-particle partitioning described in our study for organic nitrates only. We added 50 % uncertainty to this O:C ratio calculation to account for using only signal intensity for the calculation.

In response to this comment, we modified the Section 2.6 in the Methods to describe the 2D-VBS mapping along gas-particle partitioning coefficient. The results from the 2D-VBS is added to Section 3.3.3.

Section 2.5 (in Methods)

L269-318 → L284-361

2.5. Gas-particle partitioning of organic nitrates

Every compound in the atmosphere…

The partitioning of a compound *i* between the gas and particle phases can be described by the sorption of organic compounds into existing particles, which leads to the condensation of low-volatility ~~organic~~ compounds ~~(LVOC)~~ into the particle phase. **The phase partitioning of a compound *i* can be expressed as the effective saturation concentration (C_i^*). The effective saturation concentration describes the saturation concentration of a vapor over a liquid. Volatility** ~~This mechanism~~ can **also** be defined using the partitioning coefficient driven by the volatility of the compound i ($K_{p,i}$), as expressed in Eq. 6 (...). It is proportional to the particle-to-gas concentration ratio ($C_{p,i}/C_{g,i}$) and inversely proportional to the total absorptive mass (m_{tot})**; $K_{p,i}$ is thus inverse of C_i^***.

$$K_{p,i} = \frac{C_{p,i}}{C_{g,i}} \cdot \frac{1}{m_{tot}} = \frac{1}{C_i^*} \quad (6)$$

$K_{p,i}$: gas-particle partitioning coefficient driven by volatility ($m^3\ \mu g^{-1}$)
$C_{p,i}$: concentration of *i* in the particle phase
$C_{g,i}$: concentration of *i* in the gas phase
m_{tot} : total absorptive mass concentration, measured by HR-ToF-AMS ($\mu g\ m^{-3}$)
C_i^* : effective saturation concentration ($\mu g\ m^{-3}$)

~~When expressed thermodynamically in…~~
~~(...)~~
~~conversion factors: 760 Torr atm^{-1} and 10^6 µg g^{-1}~~ ***<< moved to Section 2.5.2 with modification >>***

In this study, we characterize the bulk ON in the gas phase and the particle phase under equilibrium conditions using the particle-to-gas ratio of ON (C_{pON}/C_{gON})**, the effective saturation concentration of ON (C_{ON}^*),** and the gas-particle partitioning **coefficient** of ON ($K_{p,ON}$). … We identify this equilibrium condition as when the maximum SOA concentration is reached and remains stable over time (ranging from 0.5–5 h**, with average standard deviation of ±0.3 µg m^{-3}**), based on the AMS measurements…..(...).... to compare it with the equilibrium condition.

~~We evaluated the trend in ON partitioning by differentiating the chamber experiments by daytime and nighttime conditions, as well as different VOC precursor mixtures.~~ ***<< moved to the end of the next paragraph >>***

~~We compare the observed values of $K_{p,ON}$ … Through this comparison, we can assess whether the gas-particle partitioning of the bulk ON reflects the ON composition formed from each experiment.~~ ***<< moved to Section 2.5.2 >>***

To determine C_{pON}/C_{gON}**, C_{ON}^*,** and $K_{p,ON}$, we performed two sets of calculations, using the loss corrected concentrations and the instantaneous measured concentrations (not loss corrected). … Furthermore, we also need to consider the uncertainty of **C_{ON}^* and** $K_{p,ON}$ (as one standard deviation). This uncertainty is propagated from C_{pON}, C_{gON}, and m_{tot}, detailed in Section S3.3 of the Supplement. **Finally, we evaluated the trend in ON**

partitioning by differentiating the chamber experiments by daytime and nighttime conditions, as well as different VOC precursor mixtures.

2.5.1 Two-dimensional volatility basis set (2D-VBS) mapping

The two-dimensional volatility basis set (2D-VBS) framework describes organic aerosol volatility using C_i^* and oxygenation level, thus mapping organic aerosol volatility independently from chemical structures. The oxygenation level is described by the ratio of oxygen number to carbon number ratio or O:C ratio (n_O^i/n_C^i). The 2D-VBS mapping is visualized by plotting the O:C ratio on the y-axis against the logarithm of C_i^* ($\log(C_i^*)$) on the x-axis at 300 K (Donahue et al., 2011). The organic aerosol composition based on the carbon number (n_C^i) and effective oxygen number (n_O^i) is shown to describe organic aerosol volatility as isopleths. These isopleths are calculated for saturation concentrations over a pure liquid (C_i^o), using the non-linear expression of the group contribution method for the logarithm of C_i^o ($\log(C_i^o)$) in Eq. 7.

$$log(C_i^{\,o}) = (n_C^{\,o} - n_C^{\,i}) \cdot b_C - n_O^{\,i} \cdot b_O - 2 \cdot \left(\frac{n_C^{\,o} \cdot n_O^{\,i}}{n_C^{\,o} + n_O^{\,i}}\right) \cdot b_{CO} \qquad (7)$$

We use the parameterization of group contribution method from Stolzenburg et al. (2018) to calculate the isopleths, which takes the volatility of nitrate functional group into account. The carbon number of volatility reference (n_C^o) is 25 (pentacosane usedas reference), the carbon-carbon interaction term (b_C) is 0.475, the oxygen-oxygen interaction term (b_O) is 1.4, and the carbon-oxygen non-ideality (b_{CO}) is -0.3. The $\log(C_i^*)$ spectrum is divided into semi-volatile organic compounds (SVOC) and intermediate-volatility organic compounds (IVOC) where SVOC have $-2 < \log(C_i^*) < 2.5$ and IVOC have $2.5 < \log(C_i^*) < 6$.

The observed saturation concentrations of bulk organic nitrate (C_{ON}^*) are superposed on the 2D-VBS mapping. The O:C ratio is obtained from nitrogen-containing masses signal detected by WALL-E. As the volatility of the nitrate functional group ($-ONO_2$) is similar to the volatility of the hydroxyl group ($-OH$) according to Pankow and Asher (2008), we count one $-ONO_2$ as one $-OH$ to obtain the effective O for volatility calculations. Since the chemical formula derived from the detected masses in WALL-E cannot be used to distinguish whether the nitrogen present in the compound is nitrate or non-nitrate, the O:C ratio calculated here assumes that every nitrogen in the compound is present as $-ONO_2$ and contributes to one oxygen atom in the group contribution method. Thus, for a chemical mass formula of $C_xH_yO_zN_k$, the O:C ratio is equal to $(z - 2k)/x$. The uncertainty for O:C ratio from WALL-E is approximated to be 50 %, to take into account the use of signal intensity instead of sensitivity-corrected mass to calculate the contribution of O and C.

2.5.2. Comparison with theoretical gas-particle partitioning

<< inserted from Section 2.5 with modification >>

~~When expressed thermodynamically in Eq. 7,~~**The theoretical value for $K_{p,i}$ is a function of the average temperature (T) and the vapor pressure of *i* at a given T ($p_{L,i}^o$), as well as of the composition of the organic matter (expressed as the molecular weight, MW_{om}) and the activity coefficient (ζ), which is assumed to be 1 (Eq. 8). By estimating the pure liquid vapor pressure of *i* with a given MW_{om} and ζ, $K_{p,i}$ can be theoretically calculated for a given chemical structure using a group contribution method, for example, SIMPOL.1 from Pankow and Asher (2008). The theoretically derived value of $K_{p,i}$ calculated for different organic compound structures ~~using Eq. 7~~ can be compared to the observed bulk value of $K_{p,i}$ ~~calculated using Eq. 6~~ to deduce the average volatility of the organic compounds formed (thus**

related to some possible chemical structures) and to characterize the bulk properties of the SOA mixture (Brownwood et al., 2021).

$$K_{p,i} = \frac{760 \cdot R \cdot T \cdot f_{om}}{10^6 \cdot MW_{om} \cdot \zeta \cdot p^o_{L,i}} \quad (8)$$

R: ideal gas constant (0.082 L atm K^{-1} mol^{-1})
T : average temperature (K)
fom: absorptive organic fraction of the PM
MW_{om}: average molecular weight of the organic matter (g mol^{-1})
ζ: activity coefficient of compound *i* in the organic fraction of the PM (assumed to be 1)
$p_{L,i}^o$: pure liquid vapor pressure of *i* at T (atm)
conversion factors: 760 Torr atm^{-1} and 10^6 μg g^{-1}

We compare the observed values of $K_{p,ON}$ … Through this comparison, we can assess whether the gas-particle partitioning of the bulk ON reflects the ON composition formed from each experiment.

Section 3.3.1 (in Results and discussion)

L374-376 → **L450-453**

3.3.1 Influence of daytime vs. nighttime oxidation ~~and NO~~ conditions

The particle-to-gas ratio of ON at equilibrium conditions can be used to compare the volatility of the bulk ON aerosol produced from different VOC precursor compositions in a reaction mixture **under daytime vs. nighttime oxidation conditions**, regardless of the total absorptive mass.

L501, new figure inserted (Figure 5)

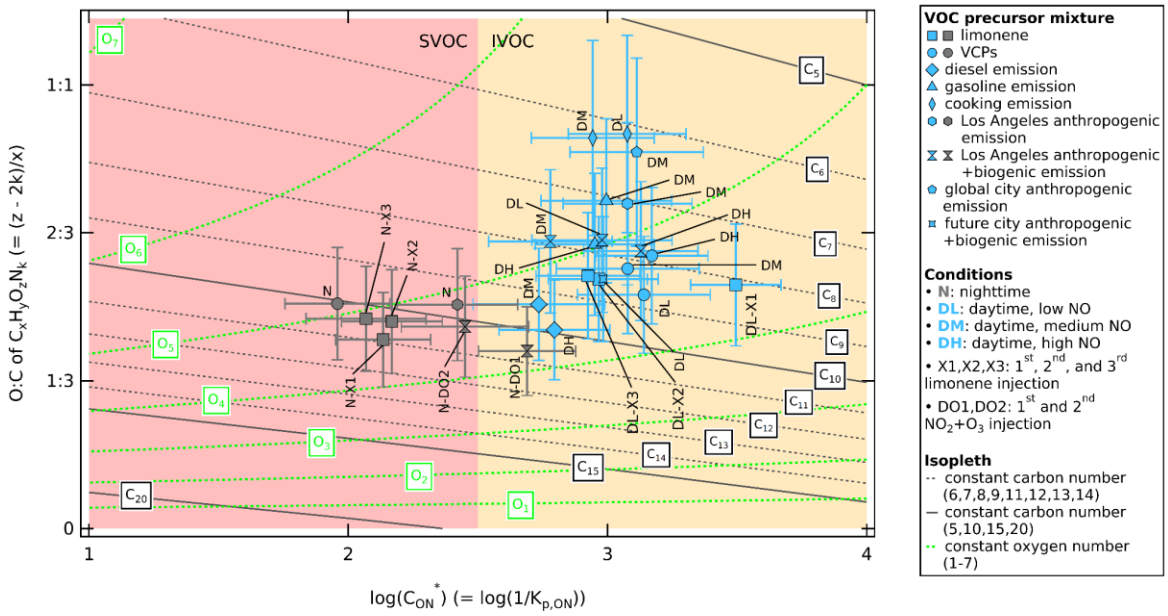

Figure 5. Two-dimensional volatility basis set mapping expressed as logarithm of effective saturation concentration of organic nitrate (log(C_{ON}^*) = log(1/$K_{p,i}$)) in a 2-D space with log(C_i^*) on the x-axis and

O:C ratio of $C_xH_yO_zN_k$ (= (z − 2k)/x) on the y-axis. The values of log(C_{ON}^*) during SAPHIR-CHANEL campaigns for various urban VOC-NO_x mixture experiments are shown color-coded by daytime (light blue) and nighttime (dark grey) conditions. The horizontal whiskers represent the uncertainty of log(C_{ON}^*) (see Section S3.3 for uncertainty propagation). The vertical whiskers represent the uncertainty from using WALL-E signal as an indication of concentration (estimated to be ±50 %). Organic composition from the group contribution method based on the carbon number (nC^i) and oxygen number (no^i) are shown to describe organic aerosol volatility as isopleths at 300 K following Donahue et al. (2011), with parameterizations following Stolzenburg et al. (2018) as described in Section 2.5.1. The dark grey lines represent carbon number isopleths and the light green curves represent oxygen number isopleths. The volatility range of semi-volatile organic compounds (SVOC) and intermediate volatility organic compounds (IVOC) are highlighted red and yellow, respectively.

L411 → new paragraph inserted, **L490-498**

The difference in C_{pON}/C_{gON} values between daytime and nighttime can be confirmed using 2D-VBS mapping, which illustrates the composition independently of temperature effects. The 2D-VBS mapping (Fig. 5) shows that the bulk organic nitrate falls within the volatility range of 2 < log(C_{ON}^*) < 4 (SVOC and IVOC). This volatility range corresponds to the volatility range of C_5 to C_{10} compounds with 4-6 effective oxygen atoms (6-8 oxygen atoms if one of the oxygen atoms represents one -ONO_2). We observe that the nighttime experiments (grey colored markers) produce lower volatility organic nitrates compared to the experiments under daytime conditions (light blue colored markers). The average volatility of nighttime organic nitrates matches heavier C_{10} compounds compared to daytime organic nitrates, which explains the higher C_{pON}/C_{gON} values for nighttime experiments as larger compounds condense more easily to the particle phase than smaller compounds, increasing the particle-phase ON concentration.

Section 4 (Conclusion)

L551 → **L675-678**

… experiments under nighttime conditions (0.030–0.137) compared to daytime conditions (0.007–0.045). **The two-dimensional volatility basis set shows that the volatility of organic nitrates ranges between 2 < log(C_{ON}^*) < 4 and matches the volatility of C_5 to C_{10} compounds, where the volatility of ON from experiments under nighttime conditions are less volatile (more similar to C_{10} compounds).** From the organic nitrate profiles, …

Section S3.3 (Supplement)

L237-242 Supplement → **L236-244 Supplement**

S3.3 Uncertainty propagation of gas-particle partitioning

The effective saturation concentration of organic nitrate (C_{ON}^*, in µg m^{-3}) is calculated using the total mass concentration of the particle phase (m_{tot}, in µg m^{-3}) and the mixing ratios of gON and pON, as shown in Eq. S17. Therefore, the final uncertainty of C_{ON}^* (σC_{ON}^*) is propagated using Eq. S18 from the uncertainties of m_{tot} (σC_{mtot}, ±20 % from AMS), gON (σC_{gON}, see Eq. S6), and pON (σC_{pON}, see Eq. S7). When expressed as log(C_{ON}^*), the uncertainty calculation follows Eq. S19.

$$C_{ON}^* = C_{gON} \cdot \frac{m_{tot}}{C_{pON}} \quad \text{(S17)}$$

$$\sigma C_{ON}{}^{*} = C_{ON}{}^{*} \cdot \sqrt{(\sigma C_{gON}/C_{gON})^2 + (\sigma C_{pON}/C_{pON})^2 + (\sigma m_{tot}/m_{tot})^2} \quad \textbf{(S18)}$$

$$\sigma \log (C_{ON}{}^{*}) = C_{ON}{}^{*}/(\ln (10) \cdot C_{ON}{}^{*}) \quad \textbf{(S19)}$$

The gas-particle partitioning coefficient of organic nitrate ($K_{p,ON}$, in m^3 μg^{-1}) is calculated using the mixing ratios of pON and gON…

RC1-M-6. A major limitation of current analysis is that several critical metrics are not quantifiable. While the manuscript presented a rich dataset, most measurements used to infer VOC consumption, ON yield, and average molecular weight are signal-based proxy without species-dependent sensitivity, fragmentation, and matrix effect. It would be helpful if the authors provide what standards were the CIMS calibrated. If any of the VOC precursors were used as calibrants, it would be helpful to better quantify the VOC consumption. Otherwise, including the uncertainty propagation from ΔVOC and average molecular weight would be helpful.

We thank the reviewer for this comment. In general, the uncertainty propagation is described in detail in the Sections S2.3-S2.7 of the Supplement. It is only briefly detailed in the main article. We reiterated where we described the sensitivities of the GC and CIMS instruments in Section 2.2.3.

L197-205 → new sentence inserted, **L206-219**

The signal intensities of different organic compounds in the gas phase (~~≈~~280 species from amine-ToF and ~~≈~~900 species from NH_4^+-Vocus) and in the particle phase (~~≈~~1000 species from WALL-E) from various mass-to-charge ratio(*m/Q*) in the observation were visualized as ON composition profile plots. ~~The ON composition profiles were characterized separately for each instrument, as each detected species may have a different sensitivity in each instrument.~~ The signals were summed from the signal intensity of compounds containing at least one nitrogen and three oxygens ($C_xH_yO_{\geq 3}N_{\geq 1}$). This criterion was chosen because it represents the minimum number of nitrogen and oxygen atoms for an ON species, but is not limited to ONs because it may also include other organic nitrogen compounds such as oxygenated amines and nitro aromatic compounds. ***<< enter new line >>***

The ON composition profiles were characterized separately for each instrument, as each detected species may have a different sensitivity in each instrument. The sensitivity of selected organic compounds is presented in Section S2.4 (MR-CIMS), and Section S2.6 (NH_4^+-Vocus) in the Supplement as a comparison. A 15 % systematic uncertainty was obtained from the calibration of MR-CIMS and we assume similar uncertainties for other gas-phase CIMS instruments. Gao et al. (2025) has described that the signal contribution of dimers of WALL-E is a factor of 2 higher compared to its mass contribution in the particle phase, and we use a 50 % uncertainty to account for this discrepancy. The ON composition distribution is an estimate of how the ON species signal is distributed across carbon and oxygen atom numbers, rather than the actual mass distribution of molecular composition.

The signal decrease of GC, MR-CIMS, NH_4^+-Vocus, and amine-ToF instruments were used to calculate ΔVOC from the amount of known injected VOCs. The sensitivity of amine-ToF, however, was not able to be characterized further. Since the uncertainty of every compound for the gas-phase instruments is not available, we used a generalized uncertainty of 15 % (obtained from MR-CIMS systematic uncertainty) to propagate uncertainty from ΔVOC for ON molar yield. This might be not very explicit in the manuscript since it was only briefly mentioned in Section 2.3 and the uncertainty propagation is detailed in the Supplement (Section S3.1).

We have reiterated this information in the manuscript to remind the reader about the uncertainty.

L212-217 → **L226-230** (avoiding repetition from the previous sentence)

> The percentage of VOC concentration that was consumed was calculated by observing the signal intensity difference of various VOCs detected by the MR-CIMS-$C_6H_6^+$ or NH_4^+-Vocus measurements between the moment of VOC injection and the steady state. The expected injected concentration of each VOC was then multiplied by the decrease in signal intensity for each compound (or compound family) to obtain the mixing ratio of consumed VOCs. The expected mixing ratios of injected and consumed VOCs ~~are calculated based on the injected volume and~~ are not verified ~~concentration~~ by **calibrated concentration** measurements.

L322-324 → **L379-382**

> In general, we observed a higher consumption of VOCs under daytime conditions compared to nighttime conditions **from the signal intensity-based observations of GC and various CIMS**. We observed ~~across experiments~~ a decrease by 96 % in average of isoprene signal/concentration under daytime conditions and 61 % under nighttime conditions.

L330-331 → **L387-391**

> With the percentage of VOCs consumed varying depending on the compound and the oxidation conditions (daytime vs. nighttime), the ON molar yields range between 2–21 % (see Table 2). **The uncertainty propagation related to the yield value is detailed in Section 2.3 and in Section S3.1 in the Supplement. These yields are derived from the calibrated observations of total NO_y, NO_x, HONO, MR-CIMS and AMS for $\Delta C_{ON,tot}$, and from the signal intensity-based observations of GC and various CIMS instruments for $\Delta C_{VOC,tot}$.** Higher yields are observed …

The uncertainty of $pRONO_2$ molecular weight (MW_{pRONO2}) is also mentioned briefly in Section 2.4 described in Section S3.2, but not in detail. It comes from the standard deviation of the average WALL-E signal when the SOA concentration is stable (range of 0.4-9.1 g mol^{-1}). This, however, was simplified and did not include the uncertainty from the WALL-E signal intensity, which is likely to be larger. The sensitivity of WALL-E was also not possible to be characterized further during the campaign. In Gao et al. (2025), they described that the signal contribution of dimers in their study (23-29 %) is roughly double compared to their mass contribution in the particle phase (14-18 %), and thus generates uncertainty.

We finally used 50 % uncertainty to approximate the entire uncertainty related to WALL-E observation in this study (including systematic and random errors). The use of 50 % uncertainty changed the reported standard deviation for MW_{pRONO2}. The average molecular weights under nighttime conditions and under daytime conditions are now reported as 330±80 g mol^{-1} and 250±30 g mol^{-1}, respectively (mean±weighted standard deviation, which includes the 50 % uncertainty and the standard deviation from the average). Furthermore, this also affects the uncertainty of $pRONO_2$ mass fraction (%). We made changes throughout the manuscript accordingly.

L9-10 → **L9-10**

> Particulate organic nitrates have a higher average molecular weight under nighttime conditions (~~331±13~~**330±80** g mol^{-1}) than under daytime conditions (~~258±24~~**250±30** g mol^{-1}) **mainly** due to ~~increased oligomerization~~ **a higher dimer fraction**.

L249-251 → **L262-265**

> This approach, however, ~~may~~ **used signal fraction rather than mass fraction of WALL-E observations to calculate the molecular weight. We used 50 % uncertainty to our bulk $pRONO_2$ molecular weight**

estimate to consider uncertainty of representing mass fraction contribution from signal intensity of WALL-E. Additionally, this approach may also include other organic nitrogen compounds such as nitro aromatic compounds, which ~~is~~ **are** also detected by WALL-E.

L265-268 → **L280-283**

We estimate the uncertainty (as one standard deviation) of the $pRONO_2$ mass fraction from the uncertainty of the determination of pNO_3 and Org in AMS (each contributes ±20 %), the NO_x^+ ratio method to obtain pON from AMS (±23 %, …), and the ~~standard deviation of the average~~ **uncertainty of** MW_{pRONO2} **(±50 %)**. The …

L351 → **L442, Table 2 caption**

Table 2. List of ON yields ~~(~~and their uncertainty~~)~~ from experiments in the SAPHIR-CHANEL 2024 campaign included in this work, which were grouped based on volatile organic compound (VOC) precursors and arranged in ascending order from low NO to high NO levels, including nighttime conditions. The yields are presented as the molar ratio of total ON formed in the gas and particle phases to the consumed VOC concentrations ($\Delta C_{ON,tot}/\Delta C_{VOC,tot}$, in %). The molecular weight **estimate** of $pRONO_2$ ($MWpRONO_2$, in g mol^{-1}) and $pRONO_2$ mass fraction to the total organic aerosol mass (OA) ($\Delta C_{pRONO2}/\Delta C_{OA}$, in %)**, including their uncertainties,** are also listed. The …

L354 → **L445, Figure 3 image and caption**

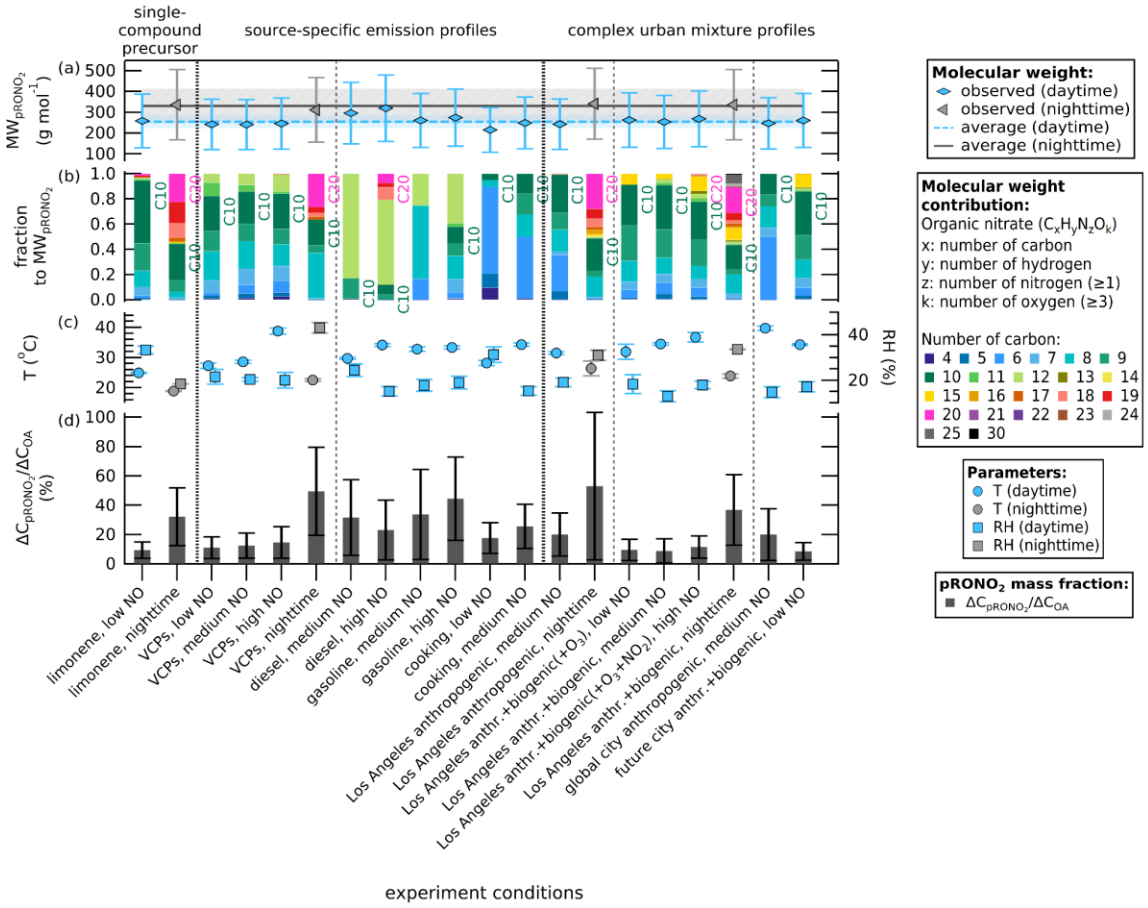

Figure 3. … precursor mixture. **The whiskers represent 50 % uncertainty from using WALL-E signal intensity instead of sensitivity-corrected mass concentration. The** plot shows an average of ~~331±13~~**330±80** g mol^{-1} for nighttime experiments and an average of ~~258±24~~**250±30** g mol^{-1} for daytime experiments (color shading represents one **weighted** standard deviation of the ~~average~~ **mean**). **(b)** Contribution fraction **based on WALL-E signal intensity** of organic compounds color coded by the carbon atom number to the molecular weight of bulk pON. **(c) Mean temperature (left y-axis, in °C) and mean relative humidity (RH, right y-axis, in %) when the SOA formation has peaked, color coded by daytime and nighttime conditions. The whiskers represent one standard deviation of the mean (0.1-2.5 °C for temperature and 0-4 % for RH). (d) Values of** pRONO$_2$ mass fraction over total OA (left y-axis, bars in %) ~~and temperature (right y-axis, in °C)~~. The whiskers represent the uncertainty of the mass fraction (one standard deviation).

L351-355 → **L421-426**

… has peaked. The summary of the molecular ~~weights~~ **weight estimates** can be found in Table 2. ~~This~~**The molecular weight estimate** is based on WALL-E observations assuming the same sensitivity for all masses detected **(50 % uncertainty included)**. It is rather a comparative approach between different experiments ~~and~~ **so** the discussion below is not affected by the fact that ~~we are not quantifying everything with WALL-E~~**the WALL-E results are not mass quantitative**. An average molecular weight of ~~331±13~~**330±80** g mol^{-1}

(mean ± weighted standard deviation) is observed for nighttime experiments, higher compared to the average molecular weight of ~~258±24~~**250±30** g mol^{-1} for daytime experiments.

L530 → **L653**

We have presented the molar yield, molecular weight **estimate**, and the gas-particle partitioning of bulk organic nitrate in …

L537-538 → **L659-661**

… based on signal intensity of chemical ionization mass spectrometer shows that the average molecular weight is ~~258~~**250** g mol^{-1} under daytime conditions and ~~331~~**330** g mol^{-1} under nighttime conditions. This difference …

L255-256 Supplement → **L224-225 Supplement**

Therefore, the uncertainty for $pRONO_2$ mass fraction is propagated from the uncertainties of pON (σ_{CpON}, see Eq. S7), molecular weight of bulk pON ($\sigma_{MWpRONO2}$, ~~depending on each experiment±~~**50 % from WALL-E**), and Org …

Minor comments (RC1-m):

RC1-m-1. Method section: how was the chamber conditioned/cleaned between experiments?

The chamber is flushed at the end of each experiment to purge any lingering gas and particles in the chamber to parts per trillion (ppt) level, and humidified at the beginning of each experiment. We added a new line at the end of Section 2.1.

L105-107 → **L110-112**

… Fig. S1 of the Supplement. A chamber experiment was started by humidifying the air **with a flow rate of 200-300 m^3 h^{-1}** until ~60 % relative humidity (RH) was reached, except for the limonene experiment under nighttime conditions, where ~~it~~**RH** was ~20 %. After about an hour…

L113 → **L119-121**

…with 1–1.5 h intervals. **At the end of each experiment, the chamber is flushed with clean synthetic air (N_2, O_2, purity >99.9999 %) at a flow rate of 150-250 m^3 h^{-1} overnight to reach mixing ratio of parts per trillion (ppt) level of various gas species (e.g., NO_x, O_3, VOCs).**

RC1-m-2. Line 108: what are the results for background experiments and how did they help with the experiments with VOC injection?

The background experiments show a low to negligible amount of gas phase ON and particle phase ON produced in the chamber, which suggests low ON formed or leached from the residual chemical species sticking to the wall of the chamber after flushing/opening the roof (contact with sunlight).

RC1-m-3. Line 249-251: as the author noted, other organic nitrogen compounds might be included, I wonder if other parameter can help exclude non-ON species? Such as N:O, DBE, etc.

The use of N:O and DBE may be useful but requires further analysis to characterize how we use this information to deduct the amount of non-ON species from the total organic nitrogen compounds.

RC1-m-4. Line 297: what activity coefficient (or assumptions) is used in the calculation?

Activity coefficient of 1 is assumed. We have added this information to the manuscript:

L285-286 → **L345-346**

> …, MW_{om}) and the activity coefficient (ζ)**, which is assumed to be 1**. By estimating the …

L297, Equation 7 → **L355, Equation 8**

> ζ: activity coefficient of compound *i* in the organic fraction of the PM **(assumed to be 1)**

RC1-m-5. Line 303: what is the criteria used to determine the "SOA concentration remains stable"? Please provide more statistical information (e.g., slope threshold, standard deviation).

We added this information to the manuscript:

L303-304 → **L305-307**

> … rate.We identify this equilibrium condition as when the maximum SOA concentration is reached and remains stable over time (ranging from 0.5–5 h**, with average standard deviation of ±0.3 µg m^{-3}**), based …

RC1-m-6. Figure 3: considering include RH information together with temperature, and include uncertainty/error bars for temperature and RH. For the legend, there is a overbar for carbon number = 10 and 20, please clarify what these denote.

We made changes as suggested in Figure 3 (see in the response to RC-1-M-6). We have moved the temperature into new plot, and added RH inside the same plot but different axis. The whiskers represent their standard deviations, which are quite small (0.1-2.5 ºC for temperature and 0-4 % for RH). The overbar (which is a "T" letter) appears for carbon number = 10 and 20 because we added extra text label of C10 and C20 in the plot. We removed them from the legend.

RC1-m-7. Line 371-372: "this could also be caused by …… in complex urban mixtures". This sentence does not seem to explain the previous conclusions, where more ON were formed for nighttime experiments, as both daytime and nighttime experiments have different VOC precursors. Please revise for clarity and logical connection.

We corrected the text as follows:

L370-372 → **L445-448**

> … concentration. This shows that despite **larger** VOCs consumption under OH. chemistry, more ON is formed in the particle phase under NO_3· chemistry. This could also be caused by the reduction in SOA formation due to interactions between the products of different VOC precursors present in complex urban mixtures **under OH· chemistry** …

RC1-m-8. Line 401: what does "larger" here mean? Higher MW or higher yield? Please specify.

We intend to say larger (amount) of SOA formation, which refers to the yield. We updated the manuscript as follows:

L370-372 → **L478-479**

> This is in line with several laboratory and chamber studies, which have shown that SOA ~~formation~~ **yield** from NO_3· oxidation of BVOCs is larger compared to SOA formed from OH· or O_3 oxidation…

RC1-m-9. Line 443-456: here the author separate all experiments into two categories, where the first one include limonene, VCP, city mixed with biogenic emission, and the second mainly include traffic and cooking emissions. The first category tends to form more dimers under nighttime conditions, while the second category tends to form high-volatility compounds. In line 461, the author draw the conclusion that BVOCs have a large impact on ON species. However, the VCP and LA anthropogenic emissions do not include BVOCs. Please refine this section.

We thank the referee for pointing out the discrepancy between these lines. It is indeed true that VCP and LA anthropogenic do not include biogenic emissions, but it has "biogenic" compounds from anthropogenic source (which is mentioned as BVOCs as well). We updated the text as follows for clarification:

L370-372 → **L556-559**

> Nevertheless, these findings give some insight that even in a very complex urban emission and changing urban emission composition (for instance Los Angeles anthropogenic+biogenic emission scenario vs**.** future city anthropogenic+biogenic emission scenario), **terpenes** ~~BVOCs~~ **(either coming from biogenic sources or anthropogenic sources like VCPs)** have a large impact shaping the ON species distribution in the bulk aerosol composition.

RC1-m-10. Line 470-471: "similarly to the trend of …… chemical species to the particle phase". This sentence is grammatically incomplete with no main clause. Please revise for clarity.

We update the sentence as follows:

L470-471 → **L569-570**

> Similarly to the trend of the particle-to-gas ratio, ~~since~~ lower chamber temperatures and higher RHs under nighttime conditions enhance the condensation of chemical species to the particle phase.

RC1-m-11. Figure S1: consider including time series for all the experiments and including RH for them.

We thank the reviewer for this comment. Adding the time series of 22 experiments in total will saturate the Supplement and would make it more difficult for the reader to find relevant information. We think the three examples of the time series are representative of other experiments that are included in this study. However, we have added the temperature and RH time series on top of the three examples of the experiments as shown in the figure below.

L21 Supplement → **L21 Supplement, Figure S1 image and caption**

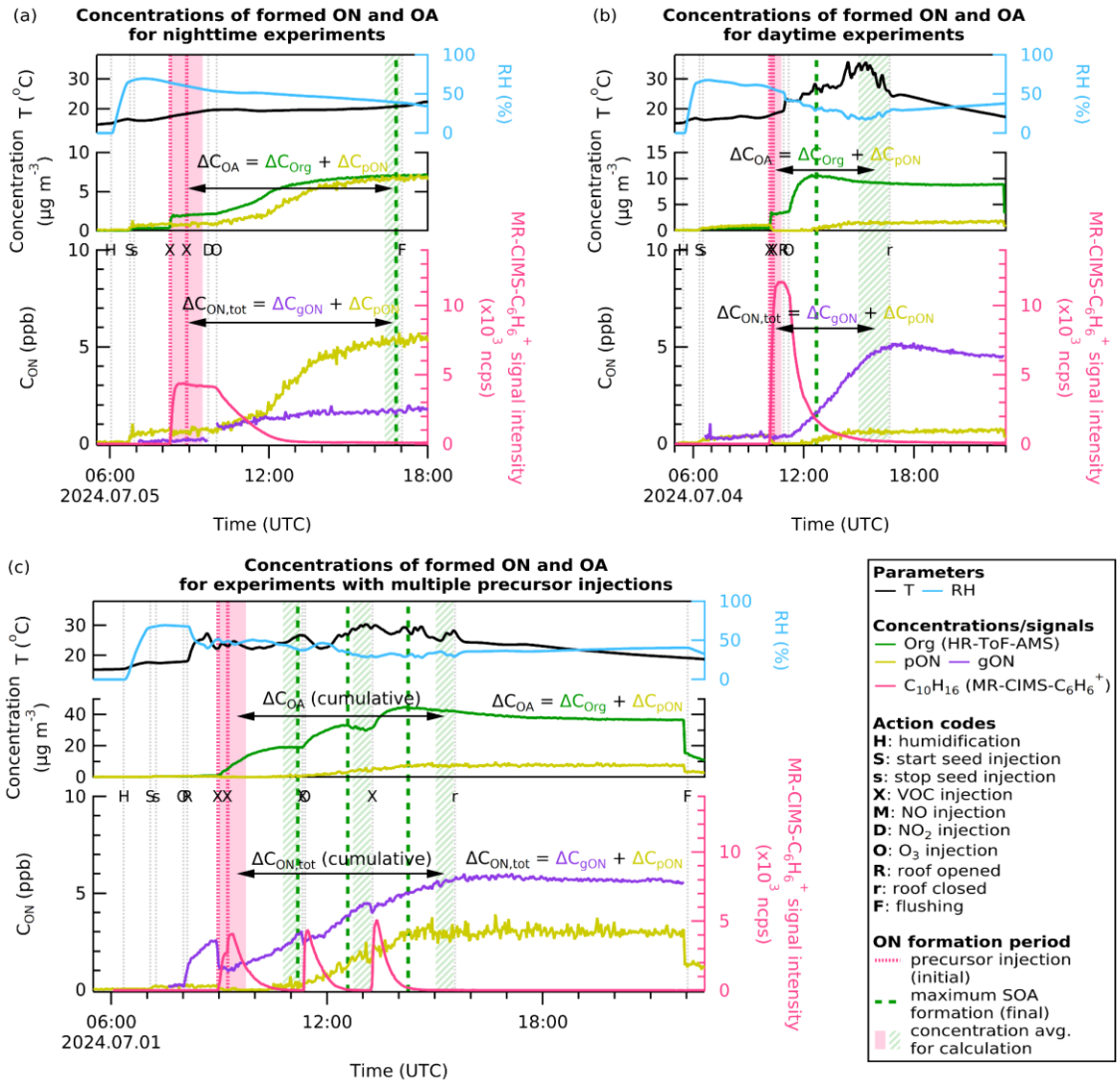

Figure S1. Time series … and **(c)** a daytime low NO experiment with limonene added at three different times. The upper left axis shows the temperature in ◦C and the upper right axis shows the relative humidity (RH) in %. The ~~upper~~middle left axis shows the total concentration …

While RH may partially influence the phase partitioning as we have stated multiple times in the manuscript, we would not like to emphasize RH as a very important factor in determining the gas-particle partitioning at this stage as it is mostly driven by vapor pressure. This also requires further study to show how the aerosol liquid water content influence the organic nitrate formation. We have included the RH when SOA formation peaked for every experiment, which was already available in line 393 and in Table S7 in the submitted Supplement.

Response to RC2 (Anonymous Referee #2): https://doi.org/10.5194/egusphere-2025-6310-RC2

Review of Nursanto et al, ACP 2026

This manuscript reports measurements of organic nitrates made during the SAPHIR-CHANEL campaign. The campaign consisted of a series of experiments made at the SAPHIR chamber looking at the oxidation of various combinations of VOCs under both photochemical and nocturnal oxidation conditions. The authors report that VOC mixtures with more unsaturated species yield more organic nitrates in the product distribution, and that nocturnal NO3-initiated oxidation yields more organic nitrates in the particle phase compared to photochemical oxidation. They also quantify the average molecular weight and the phase partitioning of the organic nitrates produced in each experiment.

Overall, the authors present an interesting dataset from a nice set of chamber experiments. I have several concerns about the analysis that I recommend the authors address prior to publication, which I have detailed below.

Major comments (RC2-M):

RC2-M-1. Quantitative isolation of the effects controlling phase partitioning of organic nitrates:

The authors report that more organic nitrates were in the particle phase during the NO_3 oxidation experiments, and they attribute part of that effect to the fact that the nighttime experiments were at lower temperatures and higher RH than the daytime experiments. But there is never any quantitative separation of these effects, nor a mechanistic explanation of the effect of RH on organic nitrate phase partitioning, both of which make the results hard to interpret in a way that is translatable to models. I recommend that the authors calculate an estimated volatility or saturation concentration (C*) distribution from each experiment to effectively control for the difference in temperature and isolate the effects of chemical / structural differences between experiments. Ultimately, to really translate the results of this nice set of experiments to models, both yields and volatility estimates are needed—and currently, yields have been provided but volatility estimates are missing.

We thank the reviewer for addressing this gap in the manuscript, which helps to improve the manuscript's quality. A similar comment has been given by reviewer #1 and has been responded to by producing an additional figure showing the C* distribution; see discussion above in RC1-M-1, RC1-M-3, and RC1-M-5.

In addition to temperature and individual compound volatility, as the authors note, the other parameter that controls phase partitioning is the total solvating (in this case, organic) aerosol mass. The authors cite Fig. S7 as evidence that differences in partitioning are not driven by differences in the total aerosol mass. But the K's shown in this figure vary by nearly two orders of magnitude, and the other effects (e.g., temperature) that contribute to partitioning coefficients aren't controlled for here, so I'm not sure that the conclusion drawn is valid. Perhaps the dynamic range of total solvating aerosol mass is small enough here that it's a relatively small effect? However, if the total solvating aerosol mass does indeed not have any effect on phase partitioning, that would imply that the system is not controlled by equilibrium partitioning theory—this would invalidate both the partitioning coefficient calculations done in this paper as well as the assumptions about organic phase partitioning in most CTMs. My suggestion earlier of estimating a volatility/C* distribution of ONs from each experiment would allow for a quantitative accounting of the effect of aerosol mass and temperature on the observed phase partitioning and hence isolation of the effect of chemical/structural differences.

We thank the reviewer for pointing out this mismatch. We agree with this explanation and we should have been more careful with the statement. Rather than arguing that solvating aerosol mass does not control partitioning, we mean to say that it does not vary enough to explain the differences in partitioning observed, similar to the NO condition where we do not see any influence of low, medium, and high NO conditions due to the relatively small range of NO_x mixing ratio during the campaign, The range of the total solvating aerosol mass (13-38 μg m^{-3}, instantaneous concentration) is typical for urban environment and within this range, the effect of aerosol mass is minimum on the phase partitioning.

We made some adjustments to the manuscript to clarify this:

L376-377 → **L453-455**

> We show in Fig. S7 of the Supplement that differences in ~~the~~ partitioning are not driven by differences in ~~the total~~ aerosol mass, **since total solvating aerosol mass only varies between 13-38 μg m^{-3} (typical concentrations of an urban environment)**. A summary of the concentrations ~~of~~ and mixing ratios used for the calculation can be found in Tables S6 and S7."

L244 Supplement → **L244 Supplement, Caption of Fig. S7**

> **Figure S7.** Scatter plot of $K_{p,ON}$ against the total absorptive mass of PM at equilibrium (m_{tot}) for various urban VOC-NO_x mixture experiments, color-coded by VOC precursor mixture. The plot suggests that differences in $K_{p,ON}$ (thus C_{pON}/C_{gON}) **in this range of total absorptive mass** are not **simply** driven by differences in m_{tot}."

RC2-M-2. Calibrated vs uncalibrated data:

If I understood correctly, the average molecular weights for the organic nitrates produced in each experiment were derived from uncalibrated speciated data. I know calibration of CIMS data can be challenging, and I agree that using it to show relative differences in the speciated distributions between experiments is useful. But deriving highly quantitative molecular weights from uncalibrated data doesn't seem quite appropriate.

We thank the reviewer for the concern regarding the molecular weight quantification described in this study. The uncertainty is indeed high if we do not consider converting the signal intensity to mass concentration based on calibration. We treat the average molecular weight of $pRONO_2$ in this study as an estimate rather than a fixed value, and try to include uncertainties when reporting the values. We have addressed this comment in the response to RC1-M-6, and have revised all reported molecular weights to rounded numbers with reported uncertainties, to emphasize that they are estimates.

Additionally, in the results section, I found myself getting confused about which quantities were derived from which instruments, which measurements were calibrated (and hence could be interpreted fully quantitatively), and which were uncalibrated (and hence should be used only for relative comparisons). If I understood correctly, C_{gON} was derived quantitatively from the NO_y instrument, C_{pON} was derived quantitatively from the AMS, and $C_{ON,tot}$ was the sum of those measurements; speciated measurements were all uncalibrated but were used to determine the average molecular weight. Quick reminders of which instruments each quantity used in the results section came from would be helpful.

The reviewer's understanding about the source of C_{gON}, C_{pON}, and $C_{ON,tot}$ are correct. We will add more reminders of which instruments are used to obtain each quantity in the results. We have updated this information throughout the manuscript as follows:

L384 → **L460-462**

> For visualization, we use a particle-to-gas ratio scatter plot (see Fig. 4), where the y-axis is C_{pON} **(obtained using NO_x^+ ratio method from calibrated AMS observation)** and the x-axis is C_{gON} **(obtained from calibrated total NOy, NOx, HONO, MR-CIMS and AMS observations)**.

L424-426 → **L511-513**

> …containing at least one nitrogen and three oxygens (which is the minimum number for an ON species), detected by various ~~chemical ionization mass spectrometer~~ **CIMS** instruments in the gas phase (by NH_4^+-Vocus and amine-ToF) and in the particle phase (by WALL-E) **detected as signal intensity**, to show the ON composition.

L465-466 → **L562-564**

> We visualize the results in this way because $K_{p,ON}$ depends on temperature. **The value of $K_{p,ON}$ is calculated based on the calibrated measurements of total NO_y, NO_x, HONO, HNO_3 (MR-CIMS), and pNO_3 (AMS).**

RC2-M-3. Mechanistic insights:

In Section 3.1, the authors note that the organic nitrate yields from limonene they measure differ significantly from those measured in previous studies, but no explanation is provided for why that might be the case. Can the authors lend some mechanistic insights into why the yields differ between studies?

We thank the reviewer for pointing out this difference. After looking more into details of the other works we cited, their yields differ because yield is defined differently in their studies, and we now clarify that in the manuscript.

If we look in details from Fry et al. (2011), the experiment setup and sequence in their study is similar to our study, and therefore the yield should be comparable. However, the 30 % ON yield for their NO_3·+limonene experiment is calculated using the total $RONO_2$ formed divided by the fraction of limonene that is consumed by NO_3·, not by the total consumed limonene. This value cannot be compared directly to the calculation of our ON yield, which includes the total consumed VOC (e.g., also by O_3). Fortunately, Fry et al. (2011) also reported the apparent nitrate yield during limonene consumption, which should be the value that we compare to because it includes all the limonene consumed, both with NO_3· and O_3. They reported the apparent nitrate yield as 15%, comparable to the ON yield we found in our study, 19 ± 3 %.

Similarly, Pang et al. (2022) calculated the 34 % ON yield in their OH·+limonene experiments as the yield of RO_2·+NO reactions from OH·-initiated RO_2· only. In their setup, they described that 60-70% of limonene are consumed through reactions with OH·, and 30-40 % from O_3. However, we do not find the value for yield taking into account the total limonene consumed.

We updated the manuscript as follows:

L334-337 → **L399-405**

> … thereby increasing the likelihood of ON formation.
> ***<< enter new line >>***

~~The daytime and nighttime limonene experiments both show 19 % yields, 11–15 % lower compared to the 34 % yield from OH+limonene experiment reported by Pang et al. (2022) and 30 % yield from NO3+limonene experiment reported by Fry et al. (2011).~~ **The daytime limonene experiment shows (19 ± 3) % yield of organic nitrate from the total consumed limonene. A similar daytime limonene experiment conducted by Pang et al. (2022) reported 34 % yield from $OH^{\cdot}$-initiated $RO_2^{\cdot}$+NO reaction, which takes into account that only 60 % of total limonene reacted. If the yield includes the other 30 % of total limonene reacted via O_3 pathway, the yield is likely to be lower since O_3 requires secondary reactions to produce $RO_2^{\cdot}$ that can react with NO to form ON. The nighttime limonene experiment shows (19 ± 4) % ON yield, similar to the 15 % total ON yield from nighttime limonene experiment reported by Fry et al. (2011) when taking into account limonene consumed by $NO_3^{\cdot}$ (50 %) and O_3 (50 %).** The cooking emission replicas …

While the information regarding the mixing ratio of O_3 has been detailed in the Table S6 of the Supplement, we think it is important to add this information in the main article to give context about the relative mixing ratio between NO_x and O_3, as a way to interpret the yield obtained in this study. We detailed this information in the response to RC2-m-4.

There are occasional references to mechanistic differences between OH and NO_3 chemistry (e.g., line 334 about unsaturated species allowing for oxidant addition and hence increasing ON formation), but without a complete mechanistic explanation for those differences. For example, why does addition vs abstraction yield more ON? And why might there be more fragmentation in the OH-initiated oxidation? Some insight from the authors on these questions would be useful.

We thank the reviewer for the constructive input. We have incorporated additional explanation regarding mechanistic differences between OH and NO_3 chemistry, as well as addition vs abstraction reactions throughout the manuscript. The changed content in the manuscript is as follows:

L334-335 → **L394-398**

… which are susceptible to addition reactions. **Electrophilic oxidants like $OH^{\cdot}$, $NO_3^{\cdot}$, and O_3 add to the carbon-carbon double bonds in unsaturated compounds. Under daytime oxidation, $OH^{\cdot}$ or O_3 addition produces a carbon radical that immediately forms $RO_2^{\cdot}$, which can react with NO_x to form organic nitrate compounds. Under nighttime oxidation, the carbon-carbon double bonds react with $NO_3^{\cdot}$ to form directly organic nitrates. The presence of unsaturated compounds** thereby increasing the likelihood of ON formation.

L355-357 → **L426-428**

… for daytime experiments. ~~The increase in dimer formation~~**We hypothesize that the increase in dimerization of $RO_2^{\cdot}$ from long-chain unsaturated VOCs (formation of $C_{\geq 10}$** compounds) and less fragmentation **or nitrate formation from short-chain $RO_2^{\cdot}$ (formation of $C_{\leq 5}$** compounds) under nighttime conditions accounts for this difference. In Fig. 3b, we see …

L448-451 → **L537-548**

<<enter new line>>
This result shows … dimer formation. **Under daytime conditions, it is likely that on top of long-chain unsaturated VOCs (e.g., compounds with $C_{\geq 10}$ like monoterpenes) in the VOC mixtures, the short-chain unsaturated VOCs (e.g., alkenes with $C_{\leq 5}$) also react with $OH^{\cdot}$ to form short-chain $RO_2^{\cdot}$. Short-chain**

RO_2· later reacts with NO_x to produce lower molecular weight ON compounds. Shorter-chain RO_2· also means that the OH·-initiated oxidation is less likely to produce compounds with high carbon atom numbers when they undergo dimerization. Under nighttime conditions, the most abundant RO_2· are likely to be from long-chain unsaturated VOCs because short-chain alkenes are less likely to react with NO_3· to produce short-chain RO_2·. These long-chain RO_2· can form organic nitrate with high carbon atom numbers through dimerization. Since dimers have lower volatility than their monomer counterparts, they are more likely to condense into the particle phase, possibly driving the higher C_{pON}/C_{gON} values for the nighttime experiments. **Furthermore, NO_3· may react with first-generation oxidation products, further oxidize low-oxygenated molecules into highly oxygenated nitrates with lower volatility, which then condense onto particles (Guo et al., 2022).**

L667-669 → **L661-663**

This difference is mainly caused by the higher contribution of heavier compounds such as dimers and lower contribution of lighter compounds ~~from fragmentations~~ during nighttime organic nitrate formation.

The authors report organic nitrate yields, which are a useful quantity that can be translated to models, and the conclusion emphasizes the importance of translating these experimental quantities to chemical transport models. However, my understanding is that, at least for the case of OH-initiated oxidation, those yields are typically implemented as a branching ratio for the RO_2+NO reaction (radical termination vs. propagation). Can the yields in these experiments be interpreted as such? Is RO_2 chemistry dominated by reaction with NO in these experiments?

The yield in this study represents the bulk ON in both gas and particle phases, and also regardless from which pathway the ON formation takes place (either through OH·-initiated or O_3-initiated RO_2· formation). This campaign is specifically designed to figure out reaction products from atmospherically relevant precursor concentrations (e.g., low NO). It means that the ON formation can include other reactions involving RO_2·, such as RO_2·+NO, RO_2·+RO_2·, RO_2·+HO_2·, and autooxidation. Thus, the yield cannot be simply regarded as the sole yield for RO_2+NO pathway.

In line 409, the authors state that the NO condition doesn't influence ON phase partitioning—but does it influence ON yield? That might be a clue about the RO_2 chemistry in these experiments.

We cannot clearly suggest whether the NO condition influence ON yield. First, the range of NO concentrations for low, medium, and high NO conditions only vary between 0.07–1.05 ppb. Second, for the same VOC precursor mixtures, most of the experiments were only performed under two NO conditions. However, if we look at experiments with VCPs and Los Angeles anthropogenic+biogenic emission mixtures as VOC precursors (where low, medium, and high NO conditions were performed), there seems to be no influence from the NO condition to the ON yield.

We have updated the manuscript to point out this information:

L338 → **L406-408**

… a yield range of 13–21 %. **The range of NO conditions in this study (0.07–1.05 ppb) is found to have no significant influence on the ON molar yield, as shown by the similar results from the low, medium, and high NO conditions of the VCP and Los Angeles anthropogenic+biogenic emission replicas.**

Minor comments (RC2-M):

RC2-m-1. Line 32: I think "dominant" rather than "prevalent" might be clearer here.

We updated the sentence as follows:

L32 → **L32**

> Although inorganic nitrate is ~~prevalent~~ **dominant**, the contribution of ambient ON is not negligible.

RC2-m-2. Line 84: Can you add a bit more of a description here of what you mean by "medium NO"?

We thank the reviewer for pointing out this in the manuscript. The "medium NO" is described in the manuscript but only later in the Methods section. The use of this term appears in the introduction before we detailed how the medium NO condition is reached. We updated the sentence as follows in the manuscript to avoid confusion.

L82-85 → **L83-85**

> A more complex urban VOC ~~NO_x~~ mixture was represented by the Los Angeles anthropogenic emission profile, which combines VCPs, cooking emissions, traffic emissions (100 % gasoline)~~, and a medium NO condition as a representation of average urban NO_x~~…

RC2-m-3. Line 97: I was a little confused when I read this line about where the NO comes from. After looking at the supplement, I think it must come from HONO, but adding a quick specification here would be helpful for the reader.

The response to this comment has been included in RC2-m-4 below.

RC2-m-4. Lines 95-100: Are the mixing ratio ranges quoted here comparing the averages between experiments or the variation within an experiment?

The mixing ratio ranges compare the averages between experiments. We updated the manuscript as follows:

L92-105 → **L92-108**

> The scenario of changing NO_x emissions and oxidation conditions …(...).... Under daytime conditions, three NO conditions were used**: low, medium, and high**. ***<<enter new line>>***
>
> The low NO condition was accomplished …(...)... This resulted in an average mixing ratio (after the roof was opened until it was closed) of 0.07-0.19 ppb of NO~~, and, of~~ 1.03–2.21 ppb of NO_2**, and 67-115 ppb of O_3 across experiments. *<<enter new line>>***
>
> The medium NO condition was achieved **from HONO photolysis** with no addition of NO and O_3 to the chamber**.**~~, leading~~ **This leads** to 0.15–0.31 ppb of NO,~~ and~~ 1.08–1.65 ppb of NO_2**, and 24-58 ppb of O_3 across experiments;**~~,~~ only slightly higher NO than for the low NO conditions. ***<<enter new line>>***
>
> To obtain high NO conditions, NO was added before exposing the chamber air to sunlight, reaching mixing ratios of 0.23–1.05 ppb of NO~~, and,~~ 2.82–4.29 ppb of NO_2**, and 62–105 ppb of O_3 across experiments**.

Lastly, the nighttime oxidation condition was achieved by adding NO_2 and O_3 to the chamber air and keeping the chamber's roof closed to block the sunlight**, leading to 10-17 ppb of NO_2 and 7-14 ppb of O_3 across experiments** and ~~to~~ favor**ing** NO_3· accumulation.

RC2-m-5. Line 108: Consider including a quantification of typical particle seed concentration at the start of experiments?

We updated the sentence as follows:

L107-109 → **L112-115**

After about an hour, ammonium sulfate ($(NH_4)_2SO_4$) was introduced as particle seeds **(concentration of ~10 µg m^{-3} and diameter of ~100 nm)** to encourage condensation into the particle phase. RH and seed type were kept constant **across experiments** to ensure the same initial aerosol conditions.

RC2-m-6. Line 123: Is a citation available for the 3 ng/m^3 LOD listed here? That seems small to me.

We thank the reviewer for pointing out this LOD value. The value of 3 ng m^{-3} was obtained from the HR-ToF-AMS manual, which refers to the typical detection limit of the instrument at 1-min time averaging.

We also have the LOD value for the ToF-AMS we deployed during the campaign. From the baseline measurements, we obtained a standard deviation of 0.015 µg m^{-3}, which translates to LOD of 0.030 µg m^{-3} at 1-min time averaging. Since we use a 2-min time averaging in this study, the LOD is 0.03*sqrt(60 s/120 s), which is equal to 0.032 µg m^{-3}. We update the value in the manuscript as follows:

L123 → **L131**

The detection limit of the instrument **from the baseline measurements at 2-min time averaging** was ~~**3 ng**~~ **0.03 µg** m^{-3}, …

RC2-m-7. Line 222: Is a citation/explanation available for gON having lower losses? Is this just the difference in wall loss rates?

In line 222, we compared the wall losses among gON, not with pON. It is likely that more volatile gON will have lower losses than less volatile gON since physically they have less adherence the wall surface due to its higher volatility.

We updated the manuscript to avoid confusion and make the statement more general for both gON and pON.

L222-223 → **L234-235**

Presumably, ON species with different volatilities, and whether they are in the gas phase or the particle phase, would have different losses. ~~For instance, it is likely that more volatile gON will have lower losses than less volatile gON.~~ **Lower volatility compounds are more likely to remain absorbed to the walls after collision than higher volatility compounds.** Here, we acknowledge this challenge which can lead to potential uncertainties in the calculation. Measured gON and pON mixing ratios are treated as bulk species.

RC2-m-8. Line 409: What is the quantitative evidence for the claim that "the NO condition in this study does not seem to influence the particle-to-gas ratio of ON"?

We can take a look at Table S7 of the Supplement, where the values of C_{pON}/C_{gON} and $K_{p,ON}$ are listed. We can pick experiments with the same VOC precursor mixture but three different NO conditions, such as VCP and Los Angeles anthropogenic+biogenic emission experiments, as shown in the Table RC2-m-8 below. Here, we can see that the values of C_{pON}/C_{gON} and $K_{p,ON}$ are not significantly different across different NO conditions for the same VOC precursor mixture. The values are also not correlated with the increasing amount of NO.

Table RC2-m-8. Comparison of C_{pON}/C_{gON} and $K_{p,ON}$ of experiments with three different NO conditions.

VOC precursor mixture	Oxidation condition	C_{pON}/C_{gON} uncorrected	$K_{p,ON}$ uncorrected (m^3 μg^{-1})
VCPs	daytime, low NO	0.008	7.00E-04
	daytime, medium NO	0.009	8.86E-04
	daytime, high NO	0.008	6.92E-04
Los Angeles anthropogenic+biogenic emission	daytime, low NO	0.013	8.66E-04
	daytime, medium NO	0.020	1.45E-03
	daytime, high NO	0.015	6.58E-04

RC2-m-9. Lines 480-485: Can you provide a little more information on how you selected the species you did the SIMPOL estimates for? I understand that the species shown correspond to observed masses and are species present in the MCM for the experimental precursors, but I would assume that there are more species than just those shown that fit those criteria, so I'm wondering how the ones shown were selected.

We thank the reviewer for this comment. We started by looking at masses that have significant signal from CIMS measurements. Based on these masses, we look at the chemical structures listed in MCM and various references in the manuscript that match the observed mass. The same mass can be derived from different family compounds (aliphatic hydrocarbons, unsaturated compounds, aromatics, biogenics, etc.). After that, we estimate their gas-particle partitioning using SIMPOL.1.

It also includes our hypothesis of plausible addition reactions for compounds that are not widely studied yet, for instance organic nitrates formed from long-chain aldehydes such as octanal and nonanal. The structures of isoprene and monoterpene dimers are also hypothetical. We attach the backbone of two monomers through a peroxide bridge and add functional groups in chemically-plausible positions within the chemical structure until the chemical formula of the structure matches some of the prevalent observed masses.

We want to point out that the compounds shown in the figure is not an exhaustive list. The compounds are just representative species to illustrate some structures corresponding to the observed volatility range, and not a complete list of expected species. We updated the caption of Figure 6 **(now Figure 7)** to further clarify:

L508, Figure 6 caption → **L605, Figure 7 caption**

> ~~**Figure 6**~~ **Figure 7.** Scatter plot of $K_{p,ON}$ against the average chamber temperature …(...)... for various ON compounds, mostly from isoprene (e.g., NISOPOOH and dimer of NISOPOOH), α-pinene (e.g., NC101CO, APINBNO3), and limonene (e.g., C928NO3, C1012NO3, LIMBNO3, NLIMOOH, LMKANO3, NLMKAOOH). The chemical structures are not observed from the measurements but based on the *m/Q*

detected by the instruments as comparison to the observed bulk $K_{p,ON}$. Chemical structures of selected ON compounds **(representative)** are shown in and below the plot.

Other changes

We also made some minor changes along the review process to clarify the text.

Abstract

L1-2 → **L1-2**: Oxidation of volatile organic compounds (VOCs) involving hydroxyl radicals ($OH^{\cdot}$)~~,~~ **and** nitrogen oxides (NO_x), or nitrate radicals ($NO_3^{\cdot}$) forms organic nitrates that undergo gas-particle partitioning, changing the lifetime of nitrogen ~~compounds~~ and their deposition on ecosystems

L12-14 → **L12-14**: Although gas-phase organic nitrate composition varies substantially between precursor mixtures, bulk organic nitrate ~~volatility~~ **partitioning** is generally similar to that of modeled oxidized monoterpene nitrates (10^{-4}–10^{-2} m^3 μg^{-1} at 18–40 °C).

L14-15 → **L14-15**: These findings improve understanding of bulk organic nitrate sources and properties in ~~a~~ complex urban environment**s**, allowing better simulations …

Section 1: Introduction

L19-22 → **L19-22**: … which include nitrogen oxides ($[NO_x] = [NO] + [NO_2]$) and NO_x reservoir species (NO_z). NO_z includes chemical species such as …, and inorganic nitrate~~s~~ (NO_3^-).

L29-31 → **L29-31**: For instance, in the Netherlands, inorganic nitrate in the form of ammonium nitrate (NH_4NO_3) makes up the majority of ambient aerosol mass …

L36-39 → **L36-40**: ~~Because~~ ONs ~~typically~~ have ~~longer~~ **variable** atmospheric multiphase lifetimes~~, 2–97~~ **ranging from 12-97** h **for non-hydrolyzable small $RONO_2$ and from 2-15 h for non-hydrolyzable isoprene and terpene nitrates** (…), ~~longer than~~ **different compared to** the lifetime of NO_x, 2–29 h (…)~~, they~~**. Thus, ONs** can modify the overall atmospheric lifetime of reactive nitrogen …

Section 2: Methods

L90-91 → **L90**: The experiments explored in this ~~study~~**paper** do not cover all the experiments performed during the SAPHIR-CHANEL campaign.

L142-143 → **L151-152**: The **external** converter is operated at 350 °C … to maximize the conversion of ONs.

L149 → **L158**: The conversion efficiency of NH_4NO_3, $(NH_4)_2SO_4$, and 2-ethylhexylnitrate (a~~n~~ ~~ON~~**$RONO_2$** compound, …

L152-153→ **L161-162**: These results are comparable … and confirm that the converter decomposes **all** pNO_3 but not NH_3 or NH_4^+.

L178-179 → **L187-188**: The multi-reagent CIMS (MR-CIMS, Vocus B2, Tofwerk AG, Switzerland)**,** ~~is~~ a newly designed instrument equipped with bipolar ToF, **is used to**~~which can~~ simultaneously measure cations and anions without inner interference.

L207-209 → **L221-223**: The ON molar yield in each chamber experiment was calculated by determining the ratio of the mixing ratio of total ON formed in both the gas phase and the particle phase ($\Delta C_{ON,tot}$) to the mixing ratio of VOC consumed ($\Delta C_{VOC,tot}$). The ON molar yield ($\Delta C_{ON,tot}/\Delta C_{VOC,tot}$) is expressed in Eq. 2.

Section 3: Results and discussion

L339-340 → **L409-410**: In contrast, experiments replicating VCPs and more complex urban emission profiles (i.e., the replica of Los Angeles city, global city, and future city emission profiles) have 2–7 % **ON molar** yields, …

L386-388 → **L465-466**: The plot shows the experiments classified based on the presence of light (daytime**, light blue**) and absence of light (nighttime**, dark grey**) conditions ~~(light blue and dark grey, respectively)~~.

L405-406 → **L483-484**: The different C_{pON}/C_{gON} values are thus inferred to be related to differences in temperature and RH in the daytime and nighttime conditions, as well as **different** ON volatilities in SOA formation caused by daytime $OH^{\cdot}$ versus nighttime $NO_3^{\cdot}$ chemistry.

L430-442 → **L517-529**: ~~We acknowledge that the composition profile may include other organic nitrogen compounds such as oxygenated amines or nitro compounds.~~ The ON composition distribution shown here is an estimate of how the ON species signal is distributed across carbon and oxygen atom numbers, rather than the actual concentrations, as each detected species may have a different sensitivity in each instrument. … The further oxidation of the ON species starting from the gas phase until they condense into the particle phase is part of SOA formation and aerosol aging, which shapes the ON composition distribution. **We note, however, that the composition profile may include other organic nitrogen compounds such as oxygenated amines or nitro compounds.**

L474**, Figure 5 caption** → **L536, Figure 6 caption**: **Figure ~~5~~6.** The ON composition profiles in the gas phase and particle phase for selected chamber experiments ... ~~Experiments replicating diesel, gasoline, and cooking emission profiles are not compared since the nighttime experiments were not conducted for these profiles.~~ **Fig. S6 shows other VOC mixtures.** The profiles show the signal fraction from the total signal

L486-488 → **L604-606**: The purpose of showing the compounds is to contextualize the **types of chemical structures consistent with observed** $K_{p,ON}$ values ~~to the chemical structures, such as the bulk ON volatility, the~~**,** and their typical oxygen number~~,~~ and ~~the~~ molecular weight**s**.

L510-511 → **L627-628**: This is interesting ~~even though~~ **since** these emission profiles do not contain any monoterpenes in the VOC precursor mixture (~50 % is alkene, and alkanes are the second highest component).

L516-517 → **L634-635**: The **ON profiles of** VCP mixture and complex urban mixtures (Los Angeles emission replicas~~) also have similar average Kp,ON values to the monoterpene-related nitrates, but the ON profiles (~~**;** see Fig. 6b,c,e,f and Fig. S6e,f) resemble more the ON profile from …

L526-528 → **L649-651**: These results ~~also~~ underscore the importance of monoterpenes in the formation of pON during SOA formation in a complex urban mixture, where the bulk volatility of ON behaves similar to monoterpenes.

L542-543 → **L665-667**: The ozonolysis chemistry may also have influence on these differences, but we expect the **observed daytime vs. nighttime** differences are **mainly** due to contrasting hydroxyl radical and nitrate radical chemistry.

Supplement

L179-180 Supplement → **L178-179 Supplement**: The ON molar yield is calculated by determining the ratio of the mixing ratio of total ON formed in both the gas phase and the particle phase ($\Delta C_{ON,tot}$) to the mixing ratio of VOC that were consumed ($\Delta C_{VOC,\mathbf{tot}}$). The ON molar yield …

References

Donahue, N. M., Epstein, S. A., Pandis, S. N., and Robinson, A. L.: A two-dimensional volatility basis set: 1. organic-aerosol mixing thermodynamics, Atmospheric Chemistry and Physics, 11, 3303–3318, https://doi.org/10.5194/acp-11-3303-2011, 2011.

Epstein, S. A., Riipinen, I., and Donahue, N. M.: A Semiempirical Correlation between Enthalpy of Vaporization and Saturation Concentration for Organic Aerosol, Environmental Science & Technology, 44, 743–748, https://doi.org/10.1021/es902497z, 2010.

Fry, J. L., Kiendler-Scharr, A., Rollins, A. W., Brauers, T., Brown, S. S., Dorn, H.-P., Dubé, W. P., Fuchs, H., Mensah, A., Rohrer, F., Tillmann, R., Wahner, A., Wooldridge, P. J., and Cohen, R. C.: SOA from limonene: role of NO3; in its generation and degradation, Atmospheric Chemistry and Physics, 11, 3879–3894, https://doi.org/10.5194/acp-11-3879-2011, 2011.

Gao, L., Zgheib, I., Stergiou, E., Carstens, C., Sari Doré, F., Dupanloup, M., Bourgain, F., Perrier, S., and Riva, M.: Characterization of the newly designed wall-free particle evaporator (WALL-E) for online measurements of atmospheric particles, https://doi.org/10.5194/amt-18-5087-2025, 2025.
Guo, Y., Shen, H., Pullinen, I., Luo, H., Kang, S., Vereecken, L., Fuchs, H., Hallquist, M., Acir, I.-H., Tillmann, R., Rohrer, F., Wildt, J., Kiendler-Scharr, A., Wahner, A., Zhao, D., and Mentel, T. F.: Identification of highly oxygenated organic molecules and their role in aerosol formation in the reaction of limonene with nitrate radical, Atmospheric Chemistry and Physics, 22, 11 323–11 346, https://doi.org/10.5194/acp-22-11323-2022, 2022.

Pang, J. Y. S., Novelli, A., Kaminski, M., Acir, I.-H., Bohn, B., Carlsson, P. T. M., Cho, C., Dorn, H.-P., Hofzumahaus, A., Li, X., Lutz, A., Nehr, S., Reimer, D., Rohrer, F., Tillmann, R., Wegener, R., Kiendler-Scharr, A., Wahner, A., and Fuchs, H.: Investigation of the limonene photooxidation by OH at different NO concentrations in the atmospheric simulation chamber SAPHIR (Simulation of Atmospheric PHoto-chemistry In a large Reaction Chamber), Atmospheric Chemistry and Physics, 22, 8497–8527, https://doi.org/10.5194/acp-22-8497-2022, 2022.

Pankow, J. F. and Asher, W. E.: SIMPOL.1: a simple group contribution method for predicting vapor pressures and enthalpies of vaporization of multifunctional organic compounds, Atmospheric Chemistry and Physics, 8, 2773–2796, https://doi.org/10.5194/acp-8-2773-2008, 2008.

Stolzenburg, D., Fischer, L., Vogel, A. L., Heinritzi, M., Schervish, M., Simon, M., Wagner, A. C., Dada, L., Ahonen, L. R., Amorim, A., Baccarini, A., Bauer, P. S., Baumgartner, B., Bergen, A., Bianchi, F., Breitenlechner, M., Brilke, S., Buenrostro Mazon, S., Chen, D., Dias, A., Draper, D. C., Duplissy, J., El Haddad, I., Finkenzeller, H., Frege, C., Fuchs, C., Garmash, O., Gordon, H., He, X., Helm, J., Hofbauer, V., Hoyle, C. R., Kim, C., Kirkby, J., Kontkanen, J., Kürten, A., Lampilahti, J., Lawler, M., Lehtipalo, K., Leiminger, M., Mai, H., Mathot, S., Mentler, B., Molteni, U., Nie, W., Nieminen, T., Nowak, J. B., Ojdanic, A., Onnela, A., Passananti, M., Petäjä, T., Quéléver, L. L. J., Rissanen, M. P., Sarnela, N., Schallhart, S., Tauber, C., Tomé, A., Wagner, R., Wang, M., Weitz, L., Wimmer, D., Xiao, M., Yan, C., Ye, P., Zha, Q., Baltensperger, U., Curtius, J., Dommen, J., Flagan, R. C., Kulmala, M., Smith, J. N., Worsnop, D. R., Hansel, A., Donahue, N. M., and Winkler, P. M.: Rapid growth of organic aerosol nanoparticles over a wide tropospheric temperature range, Proceedings of the National Academy of Sciences, 115, 9122–9127, https://doi.org/10.1073/pnas.1807604115, 2018.